ARTICLE

ACUTE LYMPHOBLASTIC LEUKEMIA

TLE4 is a repressor of the oncogenic activity of TLX3 in T-cell acute lymphoblastic leukemia

Lukas Lauwereins[1,2,6], Quentin Van Thillo[1,2,6], Sofie Demeyer[1,2], Nicole Mentens[1,2], Sarah Provost[1,2], Kris Jacobs[1,2], Olga Gielen[1,2], Lien Boogaerts[1,2], Charles E. de Bock[1,2,3], Guillaume Andrieu[4], Vahid Asnafi[4,5], Jan Cools[1,2]✉ and Alexandra Veloso[1,2]✉

T-cell acute lymphoblastic leukemia (T-ALL) is an aggressive hematological disease originating from the malignant transformation of T-cell progenitors, caused by the accumulation of genetic aberrations. One-fifth of T-ALL patients are characterized by ectopic expression of the homeobox transcription factor TLX3. However, the role of TLX3 in T-ALL remains elusive, partly due to the lack of suitable study models. Strikingly, this TLX3-positive subgroup has a high frequency of FLT3 mutations, predominantly FLT3-ITD, in pediatric cases. To investigate this, we generated ex vivo cultured pro-T cells driven by the co-expression of TLX3 and FLT3-ITD, which conferred IL7 independent growth. This model allowed us to confirm that TLX3 expression and FLT3 signaling cooperate to transform T-cells and induce an oncogenic context. Data from this cell model, combined with gene expression data from TLX3 positive T-ALL cases, revealed a strong downregulation of the transcriptional repressor TLE4. Furthermore, TLE4 showed to have a repressive effect on ex vivo TLX3 T-ALL cell growth, likely caused by a partial reversal of the TLX3 transcriptional profile. In conclusion, we developed a TLX3+FLT3-ITD pro-T cell model and used it to illustrate that TLX3 directly represses TLE4 expression, which is beneficial for the oncogenic function of TLX3.

Leukemia (2025) 39:568–576; https://doi.org/10.1038/s41375-025-02513-w

INTRODUCTION

T-cell acute lymphoblastic leukemia (T-ALL) is an aggressive hematological disease originating from the malignant transformation of T-cell progenitors caused by the accumulation of genetic aberrations [1]. The majority of patients are characterized by chromosomal translocations resulting in the ectopic expression of transcription factors, such as TAL1, TLX1, and TLX3, and additional mutations in transcriptional regulators and signaling pathways that shape leukemia development [1, 2]. Under normal circumstances, TLX3 is not expressed in the hematopoietic system but rather has a vital role in determining glutamatergic differentiation of dorsal root ganglion neurons [3]. However, in one-fifth of T-ALL cases, TLX3 is ectopically expressed, predominantly as a result of a t(5;14)(q35;q32) translocation with the *BCL11B* locus leading to aberrant TLX3 expression during T-cell development [2]. Recently, selective breakpoint location and inactivating CTCF mutations were shown to promote looping between the BCL11b enhancer and the TLX3 promotor, explaining the occurrence of these aberrations in TLX3 patients [4]. Yet, apart from selective translocation breakpoints, a simultaneous lack of promoter methylation is crucial for aberrant TLX3 expression to emerge [5]. In light of uncovering TLX3 mechanisms of action, several high-throughput assays have identified potential interaction partners, yet a few have been thoroughly validated [6]. Some examples include the transcription factor ETS1 in a leukemic context, and the CREB-binding protein in a neuronal setting [7, 8]. Based on these, few TLX3 oncogenic mechanisms were proposed, including the repression of the T-cell receptor α (TCRα) enhancer and the upregulation of miR-125b, which both lead to a differentiation arrest of developing T-cells [7, 9]. However, to date the precise functions of TLX3 in T-ALL development remains only partially characterized.

Besides scaffolding proteins and DNA-binding mediators, transcription factors multimeric complexes also comprise transcriptional regulators. One family of transcriptional co-repressors, the transducin-like enhancer of the split family (TLE1-6), is shown to be recruited by diverse transcription factors including members of essential hematopoietic transcription factor families, like RUNX, PAX, LEF1/TCF and c-MYC [10]. A unified mechanism by which this highly conserved family mediates transcriptional repression has not been determined yet. Since TLEs have been shown to interact with the amino-terminal domain of histone H3, it is believed they are able to form chromatin-associated multimeric complexes [11]. Together with the observed recruitment of histone deacetylases (HDACs) by TLE factors, a possible mechanism implies that TLE

[1]Department of Human Genetics, KU Leuven, Leuven, Belgium. [2]Center for Cancer Biology, VIB, Leuven, Belgium. [3]Children's Cancer Institute, UNSW Sydney, Sydney, NSW, Australia. [4]Institute Necker Enfants-Malades, INSERM U1151, Paris, France. [5]Laboratoire d'Onco-Hématologie, Hôpital Necker-Enfants Malades, AP-HP, Paris, France. [6]These authors contributed equally: Lukas Lauwereins, Quentin Van Thillo. ✉email: jan.cools@kuleuven.be; alexandra.bacquelaineveloso@kuleuven.be

Received: 19 September 2023 Revised: 19 October 2024 Accepted: 17 December 2024
Published online: 21 January 2025

factors indirectly promote repressive histone marks and as such inhibit transcription [12]. Apart from indirect repression via HDACs recruitment, TLE factors have also been reported to repress transcription by directly influencing basic transcription machinery like TFIIE [13]. Notably, although all members of the TLE family do converge downstream of the Wnt signaling pathway, their role in other signaling pathways varies and is unexplored for some TLE factors [10, 14]. Lastly, one family member has been shown to bind to the activation domain of the Pax2 transcription factor and preventing this the phosphorylation required for transcriptional activation [15]. The multifunctionality of this family of transcriptional co-repressors highlights the extra level of complexity in understanding the exact mechanism of transcription factor functioning. Interestingly, one member of the TLE family, TLE1, has already been described to bind and regulate TLX1, which is ectopically expressed in 10% of T-ALL patients [16, 17]. Above all, the TLX1 transcription factor structure is highly related to TLX3, suggesting a similar TLE-mediated regulation of TLX3.

The poor understanding of the TLX3 functional activity is due, in part, to the lack of suitable in vitro and in vivo models. To overcome this issue, we generated an ex vivo T-cell leukemia model driven by TLX3, which allowed us to identify TLE4 as co-repressor of TLX3 in a defined genetic background. By using this newly developed model, alongside established in vitro models, we explored the role of TLX3 and TLE4 interplay in T-ALL.

RESULTS

FLT3-ITD and TLX3 cooperate to develop an early T-cell precursor acute lymphoblastic-like leukemia

To determine recurrently mutated genes in patients with TLX3 ectopic expression, we analyzed publicly available sequencing data of two T-ALL patient cohorts: pediatric and young adult cases from St. Jude and adult T-ALL patients from GRAALL03/05 [17, 18]. Strikingly, while internal tandem duplications (ITD) in the Fms-like tyrosine kinase 3 (*FLT3*) gene were low in the pediatric cohort, all FLT3-ITD mutations ($n = 12$) occurred exclusively in the TLX3 ($n = 7$) or LMO2/LYL1 ($n = 5$) subtypes (Fig. 1A) [17]. In contrast, for the adult T-ALL cohort only one patient showed a FLT3-ITD mutation, yet this might be an underestimation as duplications of the *FLT3* gene remain difficult to determine using standard karyotyping clinical protocols [18]. To investigate a possible cooperative mechanism between TLX3 and the constitutively activated kinase FLT3-ITD, we evaluated their potential of transforming ex vivo pro-T cells to cytokine-independent growth. Primary mouse pro-T cells require the growth factors interleukin 7 (IL7), stem-cell factor (SCF), and activation of the NOTCH1 signaling pathway by Delta-like 4 (DLL4) for survival and proliferation [19]. While expression of FLT3-ITD or TLX3 alone did not change the growth properties of the cells, co-expression of TLX3 and FLT3-ITD conferred IL-7 independent growth (Fig. 1B). This was also confirmed by flow cytometry, where we observe an enrichment of the mCherry/GFP double positive population due to the cooperation of TLX3 and FLT3-ITD (Fig. S1A). Thus, we demonstrate that the ectopic expression of TLX3 requires additional mutations to induce T-cell malignant transformation, as predicted from mutational signatures found in patients.

To further characterize our TLX3 ex vivo model, we determined the transcriptomic profile of transformed TLX3+FLT3-ITD pro-T cells, collected after 14 days in culture without IL7, and identified 4876 genes to be differentially expressed in comparison to non-transduced pro-T cells originating from the same batch but cultured with IL7 (Fig. S2A). Gene set enrichment analysis (GSEA) identified a positive enrichment of "E2F Targets" and "G2M Checkpoint" related genes, suggesting that our pro-T cell model has acquired an oncogenic transcriptional profile that stimulates cell cycle progression (Fig. 1C). This oncogenic signature is corroborated by the enrichment of "MYC Targets", high levels of which are broadly present in T-ALL and have been shown to be required for T-ALL cell proliferation and leukemia-initiating cell activity [20–22] (Fig. 1C). Interestingly, among the differentially expressed genes, multiple myeloid markers such as *Mpo* and *Cd11b* were upregulated, yet simultaneously, T cell markers such as *Cd3e* and *Cd5* were significantly downregulated but still expressed (Figs. 1D and S2A) [23]. This is also confirmed by flow cytometry, where besides the stable expression of cytoplasmic CD3 (cCD3), a subset of these TLX3+FLT3-ITD pro-T cells also showed an increased expression of the common myeloid marker CD11b (74.9%) (Fig. S1D). Additionally, GSEA indicated a significant enrichment of two independent ETP-ALL signatures, hinting at a shift towards a less differentiated T-cell stage (Fig. 1E) [17, 24, 25]. Indeed, immunophenotypic staining revealed that the TLX3+FLT3-ITD pro-T cells corresponded to the DN1 stage of T-cell differentiation (CD44+, CD25−), while the regular pro-T cell cultures reflect the more differentiated DN2 stage of T-cell development (CD44+, CD25+) (Fig. S1C). Together, this suggests that TLX3+FLT3-ITD expressing pro-T cells adopt an early-thymic progenitor ALL (ETP-ALL) like state. Overall, we established a TLX3+FLT3-ITD pro-T cell model that has a transcriptional signature that corresponds to an ETP-ALL-like leukemia, a phenotype more frequently observed in pediatric TLX3+FLT3-ITD (2/6, 33.3%) T-ALL patients than in other TLX3-positive pediatric T-ALL patients (4/33, 12.1%) (Fig. S1E) [26].

TLX3 expression directly downregulates TLE4 expression

To elucidate the direct transcriptional targets of TLX3 in pro-T cells, we developed an inducible TLX3 expression vector using a Cre-LoxP system, as previously described [27, 28]. More specifically, pro-T cells expressing the Cre recombinase coupled to Estrogen Receptor (CreERT2) were transduced with a retroviral vector containing the floxed open reading frame of TLX3 cloned in the antisense orientation. Subsequent addition of 4-hydroxytamoxifen to a final concentration of 1 µM in the culture medium activated Cre which inverted the TLX3 construct to its sense orientation. After 24 h of TLX3 induction, 456 genes were differentially expressed of which 257 were up- and 199 were downregulated (Fig. 2A). Interestingly, GSEA showed a positive enrichment of the "E2F Targets" and "G2M Checkpoint" gene sets, indicating that the oncogenic transcriptional profile of our TLX3+FLT3-ITD pro-T cell model can, at least partially, be attributed specifically to TLX3 activity (Fig. S3A). Amongst the differentially expressed genes 24 h after TLX3 induction, 3 members of the TLE family were identified with *Tle4* being significantly downregulated and, *Tle2* and *Tle6* upregulated (Fig. 2A). A direct link was further demonstrated using an inducible expression system of TLX3 and the related transcription factor TLX1, where both were able to downregulate *Tle4*. Importantly, this downregulation was not observed after inducible overexpression of the transcription factor TAL1 (Fig. 2B) [28]. Similarly, our TLX3+FLT3-ITD pro-T cell model also displayed decreased *Tle4* mRNA levels, which is solely attributed to TLX3 activity and exempted from FLT3-ITD influence (Fig. S3B). In support of these observations, T-ALL cells from patients in the TLX3 subgroup, and to a lesser extent the TLX1 subgroup, also express low levels of *TLE4*, compared to all other T-ALL subgroups. This was true for both pediatric and young adult (St. Jude) as well as adult T-ALL patients (GRAALL03/05) (Fig. 2C) [17, 18]. Both TLX3-positive T-All patients and TLX3 ex vivo model show a down-regulation of *TLE4* expression strongly suggesting TLE4 to be an important factor in this leukemia subgroup. Notably, *Tle2* which was upregulated after 24 h of TLX3 expression in pro-T cells, likewise showed a higher expression in the TLX3-positive pediatric patients (Fig. S3C). In contrast, no differences in *TLE6* expression were observed between pediatric T-ALL subgroups, despite Tle6 being upregulated after 24 h of TLX3 induction in pro-T cells (Fig. S3D).

To determine TLX3 target genes and their effect on TLE4 in a human T-ALL context, we performed ChIP-seq analysis in the human TLX3-positive T-ALL cell lines, DND41 and HPB-ALL, which indicated that TLX3 binds to the promoter region and intron 3 of *TLE4*, respectively (Fig. 2D). Based on the DepMap database, TLE4

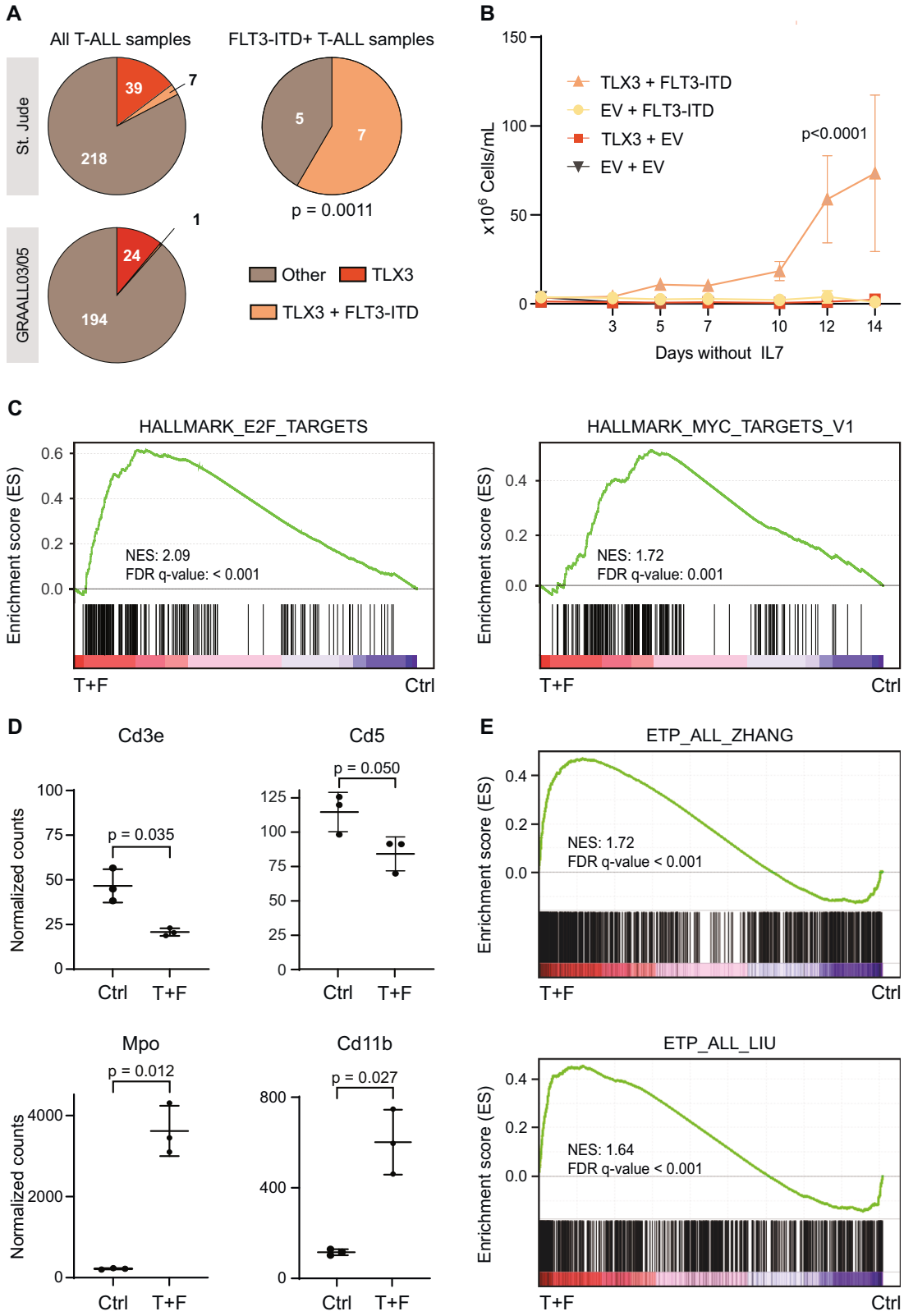

Fig. 1 FLT3-ITD and TLX3 cooperative ex vivo model represents early stage TLX3 positive phenotype. A Pie chart representing the proportion of TLX3-positivity in all T-ALL cases (left) and in FLT3-ITD positive cases (right) for pediatric and young adult (St. Jude) and adult patients (GRAALL03/05) [17, 18]. **B** Growth curve of pro-T cell cultures in the absence of IL7 after transduction with the indicated constructs. $n = 3$, p values calculated using two-way ANOVA with Tukey's multiple comparisons correction. **C** Gene Set Enrichment Analysis (GSEA) for designated gene sets of FLT3-ITD+TLX3-V5 transformed versus wildtype pro-T cells differential gene expression analysis. NES normalized enrichment score. **D** Normalized counts of indicated genes in wildtype (Ctrl) and TLX3-V5+FLT3-ITD transformed pro-T cells (T+F) are shown as mean ± SD. $N = 3$, p values calculated using Welch's t-test. **E** GSEA plots for the indicated gene sets of FLT3-ITD+TLX3-V5 transformed versus wildtype pro-T cells.

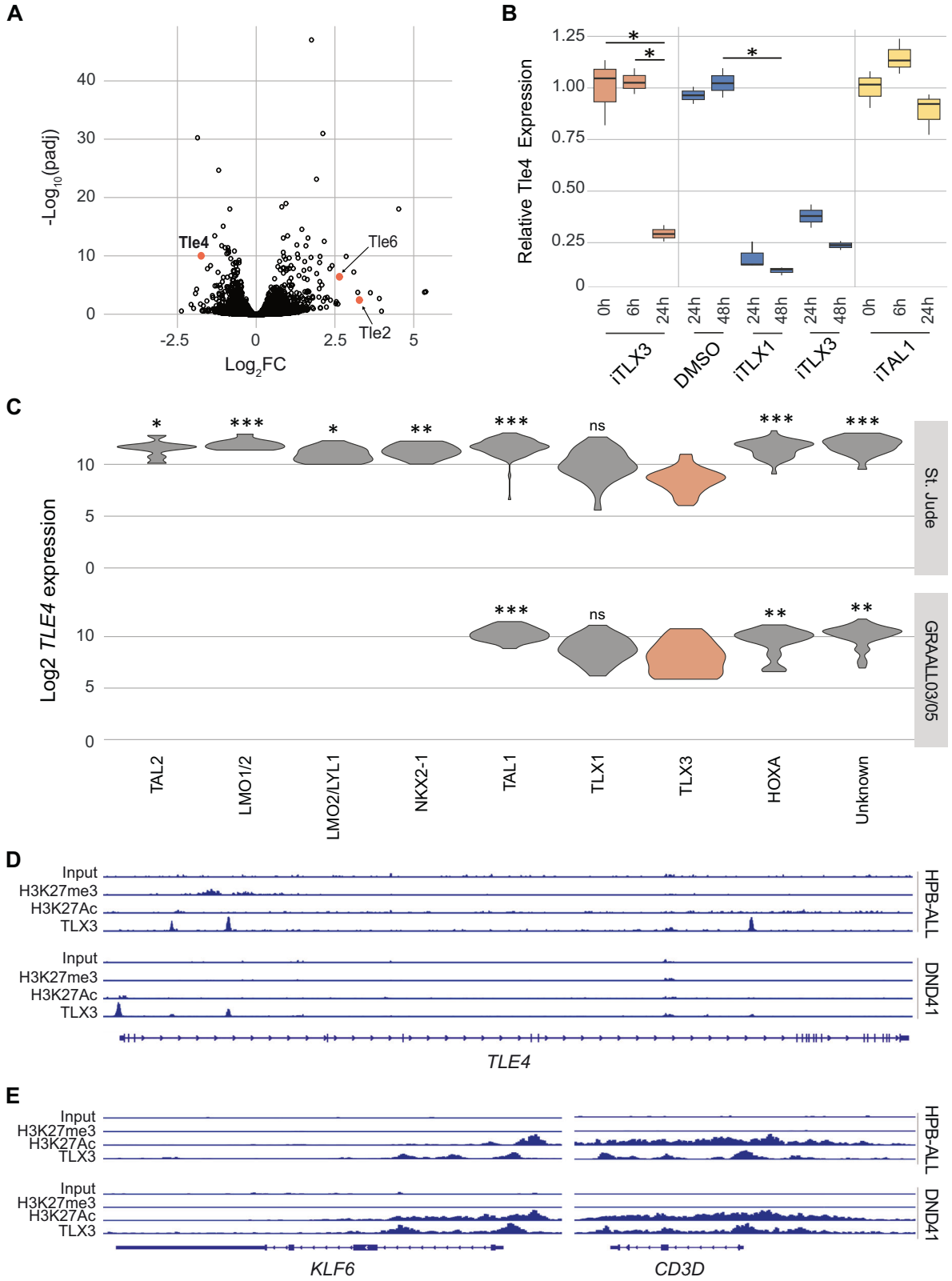

expression is low in DND41, however in HPB-ALL cells it is virtually non-existent [29]. Accordingly, ChIP-seq data show that the TLE4 gene body is absent from Histone 3 Lysine 27 acetylations (H3K27Ac) in both cell lines and show subtle Histone 3 Lysine 27 trimethylation (H3K27me3) at intron 3 in HPB-ALL. Comparison with highly expressed genes such as *KLF6* and *CD3D*, that possess pronounced H3K27Ac around their transcription start site, further corroborate the low expression of *TLE4* in TLX3 T-ALL cell lines (Fig. 2D-E). Together with the downregulation of *Tle4* mRNA levels after 24 h of TLX3 expression, this substantiates that *TLE4* transcription is directly repressed by TLX3.

Fig. 2 Downregulation of the co-repressor *TLE4* is favorable for TLX3 oncogenic activity. A Volcano plot showing differentially expressed genes of CreER pro-T cells 24 h after activating *TLX3* expression, compared to timepoint 0. *Tle* genes are highlighted in orange. $N = 3$ for each condition **B** Relative *Tle4* expression after inducing expression of TLX3, TLX1, or TAL1 in CreER pro-T for indicated timepoints. (data of TAL1 experiment from Thielemans et al. [28]). $N = 3$ for each condition. p values were calculated using Repeated measures one-way ANOVA with Tukey's multiple comparisons correction (24 h induction of TLX3) or using a Kruskal–Wallis test with Dunn's multiple comparisons correction (24 h and 48 h induction of TLX1 and TLX3). Ns non-significant, $*p < 0.05$, $**p < 0.001$, $***p < 0.0001$. **C** Violin plot showing expression levels of *TLE4* in indicated subgroups of pediatric and young adult (St. Jude) and adult (GRAALL03/05) T-ALL patients [17, 18]. Significance levels are displayed per subgroup in comparison to the TLX3 subgroup and p values were calculated using a Kruskal–Wallis test with Dunn's multiple comparisons correction. Ns non-significant, $*p < 0.05$, $**p < 0.001$, $***p < 0.0001$. **D** ChIP-seq track for TLE4 gene showing TLX3 binding, H3K27Ac, and H3K27me3 profile in DND41 and HPB-ALL cells. **E** ChIP-seq track for KLF6 and CD3D gene showing TLX3 binding, H3K27Ac, and H3K27me3 profile in DND41 and HPB-ALL cells.

TLE4 represses the oncogenic function of TLX3 through its engrailed homology 1 domain

The TLE family of transcriptional regulators are known to interact with a range of transcription factors including homeobox proteins, and act as transcriptional co-repressors [10]. The transcription factor TLX1, which shares an amino acid sequence homology of 60% with TLX3, has been shown to interact with TLE1, another member of the TLE family. Moreover, the binding between TLX1 and TLE1 could be disrupted through a point mutation in the engrailed homology (Eh1) domain of TLX1 [16]. Regarding TLX3, interactions with three TLE family members—TLE1, TLE3, and most notably TLE4—have been identified through a high-throughput proximity biotinylation assay conducted in HEK293T cells [6]. To investigate whether TLE4 can also regulate the oncogenic activity of TLX3, we generated a point mutation in the Eh1 domain of TLX3 converting phenylalanine at position 18 to glutamic acid (TLX3(F18E)) (Fig. 3A). We hypothesize that this mutation corresponding to the Eh1-domain mutation in TLX1 might prevent TLE4 repressive effect on TLX3 through direct interaction. In one directional co-immunoprecipitation assay, we pulled down TLE4 and showed a direct interaction with TLX3, which was abrogated in the event of the F18E mutation in the Eh1-domain of TLX3 (Fig. S1A). The large molecular weight of TLE4, resulting in steric hindrance for TLX3 targeting antibodies, may be attributed to the difficulty to display the interaction of TLE while pulling down TLX3.

To evaluate the effect of this mutation in TLX3 and the subsequent dysfunctional Eh1-domain, we expressed FLT3-ITD in conjunction with TLX3(F18E) or wild-type TLX3 in pro-T cells. Similar to TLX3+FLT3-ITD pro-T cells, TLX3(F18E) and FLT3-ITD co-expressing (TLX3(F18E)+FLT3-ITD) pro-T cells partially expressed CD11b (56.9%), while still retaining their T-cell nature (Fig. S1D). In the absence of IL7, TLX3(F18E)+FLT3-ITD cells proliferated faster compared to TLX3+FLT3-ITD cells (Fig. 3B). Conversely, introducing exogenous TLE4 into pro-T cells co-expressing FLT3-ITD and TLX3, resulted in decreased cell proliferation 11 days after IL7 depletion. In contrast, no substantial alteration of growth was observed in pro-T cells co-expressing TLX3(F18E) and FLT3-ITD indicating that TLE4 has a direct inhibitory role on TLX3 (Fig. 3B). Together, these data indicate that the co-factor TLE4 represses the oncogenic effect of TLX3, which is mediated by the interaction with its Eh1-domain.

TLE4 expression inverts the oncogenic effect of TLX3 on transcriptional level

To determine transcriptional changes induced by TLX3 or TLE4, RNA was extracted from the TLX3+FLT3-ITD pro-T cell model with or without overexpression of TLE4. We identified 622 differentially regulated genes by comparing TLX3+FLT3-ITD plus TLE4 overexpression and TLX3+FLT3-ITD plus empty vector (EV) (Fig. 3C), based on which, GSEA analysis revealed a positive enrichment of "TNF Signaling via NFkB" (Fig. 3D). More interestingly, GSEA analysis of "E2F Targets" and "G2M Checkpoint" gene sets that were previously enriched in the TLX3+FLT3-ITD pro-T cell model, were now negatively enriched as a consequence of TLE4 overexpression (Figs. 3D and S4B), indicating that TLE4 is able to reverse the transcriptional profile induced by TLX3.

To explore this further, we compared the transcription profiles of TLX3+FLT3-ITD versus EV+FLT3-ITD pro-T cells, identifying 8622 differentially expressed genes as result of TLX3 expression (Fig. 4A, B). Subsequently, we evaluated the influence of TLE4 overexpression on these genes by analyzing the 622 differentially expressed genes associated with TLE4 overexpression from Fig. 3C. From these 622 TLE4 regulated genes, 449 genes were specific to TLX3 and most of these genes were up and down-regulated in the opposite way when TLE4 was overexpressed compared to their expression as consequence of TLX3 alone.

In comparison to FLT3-ITD alone, 225 genes were upregulated by the co-expression of TLX3. However, upon expression of TLE4, these same genes were downregulated ("Down by TLE4"), whereas 51 were downregulated by TLX3 and subsequently upregulated by TLE4 ("Up by TLE4') (Fig. 4B). This strongly indicates that for these specific genes, TLE4 counteracts the function of TLX3 at the gene expression level. The relevance of these genes as TLX3 target genes was highlighted by TLX3 peaks found in their gene body in DND41 and HPB-ALL ChIPseq data (Fig. S4C). Of note, TLE4 overexpression did not alter the expression of T cell markers (Cd3e and Cd5) nor myeloid markers (Mpo and Cd11b) present in the TLX3+FLT3-ITD pro-T model, suggesting no alteration in cell immunophenotype induced by TLE4 expression (Fig. S3E). Together, these data highlight that overexpressing TLE4 in TLX3+FLT3-ITD pro-T cells reduces their growth potential, most likely by counteracting the TLX3 induced transcription profile, which is important for inducing a leukemic state.

DISCUSSION

In this study we generated the first ex vivo TLX3 T-ALL model with an immunophenotypic and transcriptional profile similar to ETP-ALL patients. As ectopic expression of TLX3 on its own does not lead to a leukemic phenotype, we investigated the mutational landscape of TLX3 patients and found that FLT3-ITD mutations are more common in these patients. Moreover, these aberrations, i.e., ectopic expression of TLX3 and FLT3 mutations, are often encountered in ETP-ALL patients [17, 30]. Accordingly, in our pro-T cell model the oncogenic cooperation between TLX3 and FLT3-ITD leads to an immature phenotype by expressing early myeloid markers (*Cd11b* and *Mpo*) and reducing the expression of well-known T-cell markers (*Cd3* and *Cd5*). Furthermore, we could confirm the leukemic state of our T-ALL model by the positive enrichment of E2F targets, MYC targets and G2M checkpoint related genes, next to an ETP-ALL gene signature.

A previous study performed by Renou et al. described the effect of transducing primary human T cells with TLX3 encoding viral vectors, showing that it impairs the differentiation of these cells. However, the ectopic expression of transcription factors in T-ALL is considered an initiating step in leukemia development, while additional mutations are required to fully transform from normal T cells to leukemia cells [1]. Therefore, our model is the first to describe the effect of TLX3 in a leukemic-like transformed state (IL7 independent growth) [9]. In conclusion, we developed the first ex vivo TLX3 T-ALL model, by introducing both TLX3 and FLT3-ITD, which resembles ETP-ALL patients.

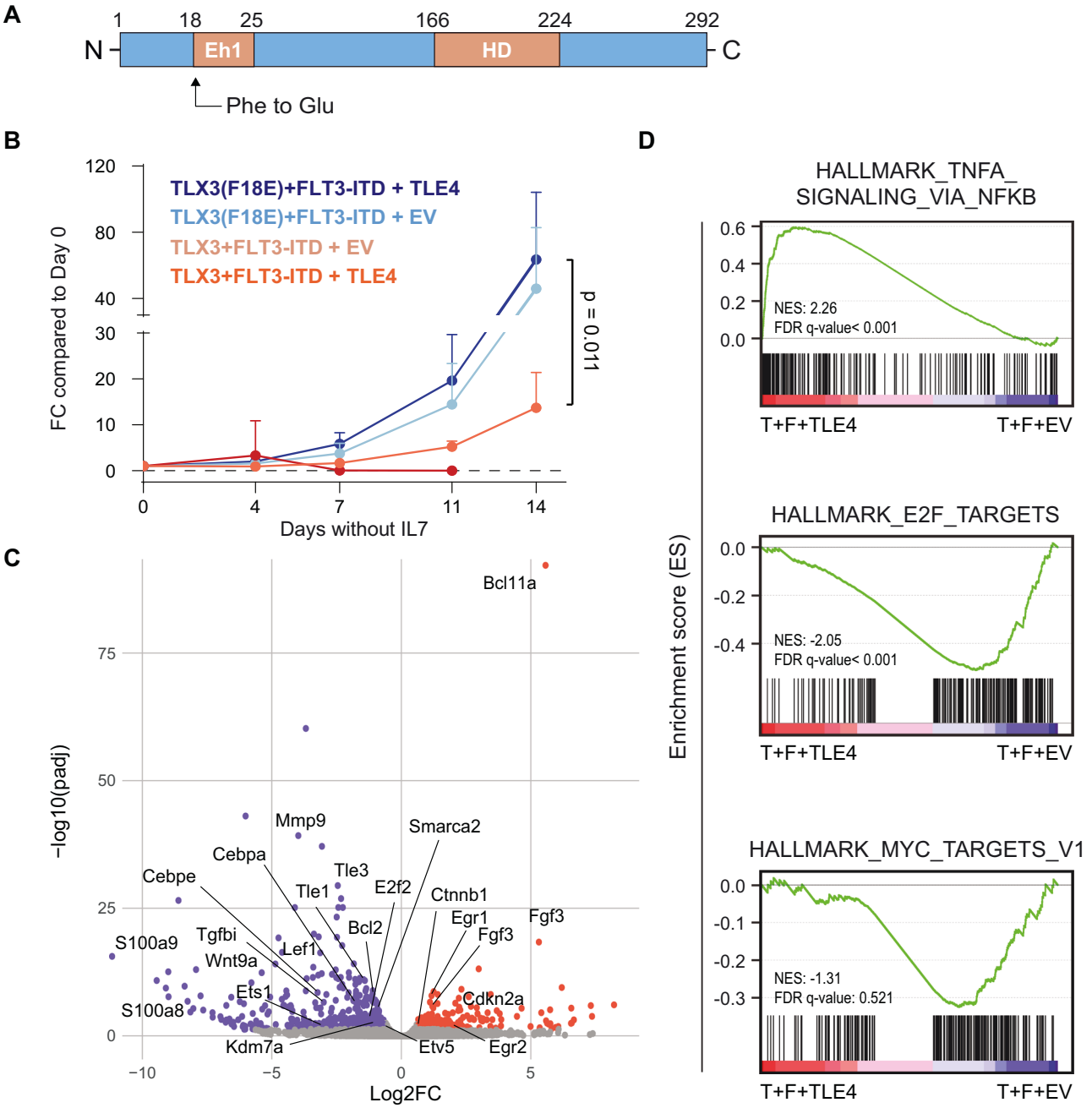

Fig. 3 TLX3 oncogenic function is repressed by TLE4 through its interaction with the EH1 domain of TLX3. A Schematic representation of the human TLX3 protein indicating its main domains and mutation site. Eh1 engrailed homology 1, HD Homeodomain **B** Growth curve of pro-T cells in the absence of IL7 after transduction with the indicated constructs. Fold change (FC) of number of cells compared to day 0 is calculated per replicate. $N = 6$ for each condition. Mean ± SD is shown. *p*-value was calculated using Friedman's test with Dunn's multiple comparisons correction. **C** Volcano plot of the differential gene expression analysis on RNA-sequencing of TLX3+FLT3-ITD+TLE4 compared to TLX3+FLT3-ITD+EV pro-T cells. Significantly up- and downregulated genes are highlighted in red and blue, respectively. $N = 3$ for each condition. **D** GSEA plots for designated gene sets of differential gene expression of TLX3+FLT3-ITD+TLE4 (T+F+TLE4) compared to TLX3+FLT3-ITD+EV (T+F+EV) pro-T cells.

Interestingly, among the downregulated genes found within our model is the transcriptional co-repressor TLE4, which mirrors the gene expression pattern found in TLX3-positive T-ALL patients, that also show the lowest TLE4 expression of all T-ALL subgroups. Using an inducible TLX3 expression strategy in mouse pro-T cells, supplemented with ChIP-sequencing in human T-ALL cell lines, we identified TLE4 as a direct transcriptional target of TLX3. Additionally, we showed that TLE4-mediated repressive effect on the growth of our ex vivo TLX3 T-ALL cell is dependent on the Eh1 domain of TLX3. Lastly, we highlight that exogenously overexpressing TLE4 in our ex vivo TLX3 model was also able to partially reverse the transcriptomic profile induced by TLX3.

In this paper, we show that introducing a single point mutation in the Eh1 domain of TLX3 can confer a substantial growth advantage to mouse ex vivo TLX3 + FLT3-ITD pro-T cells, which prevents TLE4 repressive action and results in a growth advantage. Although, we cannot rule out that the point mutation has additional effects on TLX3 itself or potential

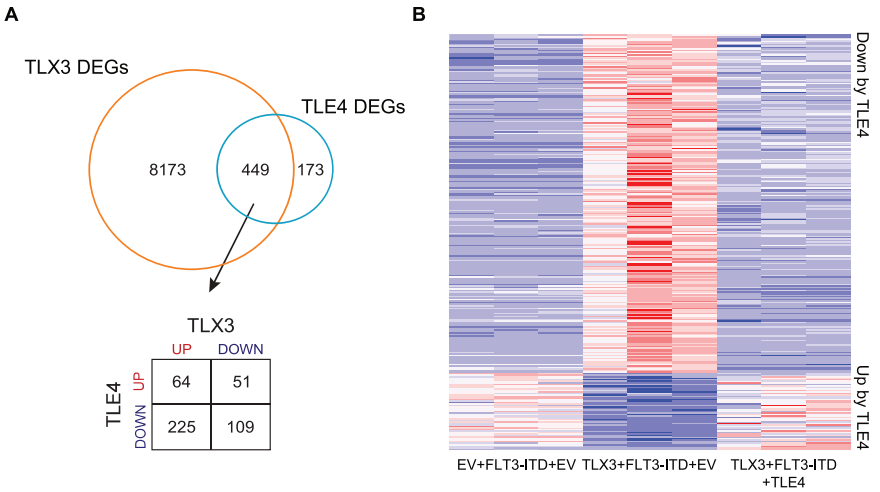

Fig. 4 TLE4 overexpression partially inverts transcriptomic changes induced by TLX3. A Graphic schematic explaining the setup of data analysis. TLX3 DEGS differentially expressed genes (DEG) in TLX3+FLT3-ITD vs EV+FLT3-ITD comparison, TLE4 DEGS DEG in TLX3+FLT3-ITD +TLE4 vs TLX3+FLT3-ITD+EV comparison **B** Heatmap of "TLX3 effect" genes that are oppositely regulated when overexpressing TLE4.

interacting partners, the importance of the Eh1-domain for the interaction of transcription factors (including homeobox proteins) with TLE (groucho) factors has been reported in literature [31, 32].

Given that we showed TLE4 negatively impacts TLX3 activity by partially reversing the TLX3-induced transcriptional profile, we would expect finding TLX3 mutations that disrupt TLE4 action in T-ALL patients. However, no record was found in cancer patient cohorts of any similar Eh1 mutation in TLX3 patients, suggesting that the downregulation of TLE4 is sufficient to obtain a favorable environment for TLX3 oncogenic activity in T-ALL. Putatively, the TLX3-TLE4 regulatory axis could be exploited therapeutically by increasing TLE4 levels to inhibit the oncogenic function of TLX3 in TLX3-positive T-ALL patients.

Besides downregulation of Tle4, we saw a significant upregulation of Tle2 after 24 h of TLX3 inducible expression in ex vivo pro-T cells, a trend which was also noticeable in T-ALL patients. Additionally, overexpressing *TLE4* in our TLX3 + FLT3-ITD pro-T model showed downregulation of *Tle1* and *Tle3* suggesting that a feedback loop involving multiple Tle family members might be present.

Overall, this study underscores the importance of developing relevant oncogenic models that recapitulate patients' mutational profiles to provide a greater understanding of the transcription deregulation found in different T-ALL subgroups. These models can then be used to unravel the mechanisms by which leukemia develops, as we showed here for TLE4.

MATERIALS & METHODS

Pro-T cell culture and growth curve

Pro-T cell cultures were established as described [19, 33]. Pro-T cells were cultured on non-treated tissue culture plates (BD Falcon #734-0949) that were first coated overnight with 10 µg/mL anti-Fc (Abcam, ab1927) in PBS and subsequently coated overnight with 2 µg/mL DLL4 (in-house production at the VIB Protein Core) in RPMI 1640 medium (Invitrogen) with 20% Fetal Bovine Serum (FBS)(Sigma-Aldrich). Cells were cultured in RPMI 1640 medium (Invitrogen) with 20% FBS (Sigma-Aldrich), mIL7 20 ng/mL (Biolegend, #577806), mSCF 20 ng/mL (PeproTech, #250-03) and Primocin 100 µg/mL (Invivogen, ant-pm-2). To establish a growth curve, the cell number and percentages of fluorescence signals were measured in technical triplicates using the MACSQuant® VYB flow cytometer (Miltenyi Biotec).

Inducible expression in pro-T cells

Inducible gene expression vectors were designed as previously described [27, 28]. Hematopoietic stem and progenitor cells (HSPC) were isolated from Rosa26-CreERT2 knock-in transgenic C57BL/6 mice to establish CreERT2 expressing pro-T cells. After spinfection of CreER pro-T cells with inducible retroviral vectors, 1 µM of 4-hydroxytamoxifen (H7904, Sigma Aldrich) was added to the culture medium. Twenty-four and 48 h after induction, RNA was extracted as previously described in this section.

Co-immunoprecipitation of TLX3 and TLE4

HEK293T cells were co-transfected with TLE4 and TLX3 expression vectors. Fluorescence signal was evaluated to assess transfection efficiency. After 24 h, cells were lysed using 1X Cell Lysis buffer (Cell Signaling Technology, 9803S) supplemented with cOmplete™ EDTA-free Protease Inhibitor Cocktail (Roche, 11873580001). Afterwards, protein concentration was determined using the Colorimetric Protein Assay Kit (Bio-Rad, #5000001) with 595 nm absorbance detection facilitated by the Perkin Elmer Victor X4. Per immunoprecipitation, 1000 µg of protein lysate was first cleared by incubation with DynaBeads protein G (Invitrogen, 10004D) for 2–3 h at 4 °C with rotation. Simultaneously, per immunoprecipitation, 50 µL of DynaBeads were coupled with 1 µg antibody by incubation in cell lysis buffer, for 1 h at RT with rotation. The following antibodies were used: HSV antibody (NB600-513, Novus Biologicals), normal rabbit IgG (#2729S, Cell Signaling) and Normal Goat IgG Control (AB-108-C, R&D Systems). The TLX3 targeting antibody was custom made by immunizing rabbits with the recombinantly produced His-tagged TLX3 protein and was kindly provided by Dr. Müller (MDC). Afterwards, coupled Dynabeads were washed with cell lysis buffer and incubated with cleared protein lysates. Immunoprecipitation was done overnight at 4 °C with rotation. After 4 washing steps with cell lysis buffer, beads were resuspended in 1X NuPAGE LDS sample buffer (Invitrogen, NP0007) and heated to 70 °C for 10 min to ensure elution of proteins. Subsequently, 10% input and IP samples were analyzed by western blot assay as previously described [25].

Chromatin immunoprecipitation (ChIP) sequencing and ChIPmentation

ChIPmentation/ChIP-seq on human T-ALL cell lines was carried out as described with modifications [34]. Briefly, 20–40 million cells were washed in PBS and cross-linked with 1% formaldehyde (Sigma-Aldrich, F8775) for 10 min at room temperature and then

quenched by addition of glycine (125 mmol/L final concentration). For nuclei isolation, cells were resuspended in 1× RSB buffer (10 mmol/L Tris, pH 7.4, 10 mmol/L NaCl, 3 mmol/L $MgCl_2$) and left on ice for 10 min to swell. Cells were collected by centrifugation and resuspended in RSBG40 buffer (10 mmol/L Tris, pH 7.4, 10 mmol/L NaCl, 3 mmol/L $MgCl_2$, 10% glycerol, 0.5% NP40) with 1/10 v/v of 10% detergent (3.3% w/v sodium deoxycholate, 6.6% v/v Tween-40). Nuclei were collected by centrifugation and resuspended in $L3B^+$ buffer (10 mmol/L Tris-Cl, pH 8.0, 100 mmol/L NaCl, 1 mmol/L EDTA, 0.5 mmol/L EGTA, 0.1% Na-Deoxycholate, 0.5% N-Lauroylsarcosine, 0.2% SDS). Chromatin was fragmented to 200–400 bp using 20 cycles (30 s on, 30 s off, High Setting) using the Bioruptor (Diagenode). Chromatin immunoprecipitation was carried out overnight in the presence of custom TLX3 antibody (provided by Dr. Müller, MDC Berlin) coupled to magnetic protein A/G beads (Millipore). Tagmentation and library preparation was carried out as previously described [34]. DNA was purified using triple-sided SPRI bead cleanup using 1.0X, 0.65X, and 0.9X ratios (Agencourt AMPure Beads, Beckman Coulter) and analyzed by Illumina HiSeq 2000 (Illumina). Raw sequencing data were mapped to the human reference genome (GRCh38/hg38) using HISAT2 (v2.2.1). Peak calling was performed using the Model-based Analysis of ChIP-Seq (MACS) algorithm (v2.2.7.1). Further analysis was performed with the deepTools package (v3.5.0).

Ethics approval

All methods were performed in accordance with KU Leuven guidelines and regulations. Pro-T cell cultures extraction from C57BL/6 mice were approved and supervised by the KU Leuven ethical committee and conducted according to EU legislation (DME-030/2023)

Both patient cohorts, St. Jude and GRAALL03/05, were detailed in prior publications [17, 18]. St. Jude cohort included 264 samples from children and young adults, with banked diagnostic and remission material from the Children's Oncology Group Study of T-ALL (NCT00408005). The study was approved by the St. Jude Children's Research Hospital Institutional Review Board, with informed consent obtained from all participants or their legal guardians [17].

For cohort GRAALL03/05, informed consent was obtained at enrollment. All trials adhered to the Declaration of Helsinki and were approved by local and multicenter research ethics committees. The GRAALL-2003 and -2005 (GRAALL03/05) studies were registered at ClinicalTrials.gov (NCT00222027, NCT00327678).

DATA AVAILABILITY

Raw RNA-seq and ChIP-seq data performed during this study can be obtained from GSE241640.

REFERENCES

1. Girardi T, Vicente C, Cools J, De Keersmaecker K. The genetics and molecular biology of T-ALL. Blood. 2017;129:1113–23. Mar 2
2. MacLeod RAF, Nagel S, Kaufmann M, Janssen JWG, Drexler HG. Activation of HOX11L2 by juxtaposition with 3′-BCL11B in an acute lymphoblastic leukemia cell line (HPB-ALL) with t(5;14)(q35;q32.2). Genes Chromosomes Cancer. 2003;37:84–91. May 1
3. Cheng L, Samad OA, Xu Y, Mizuguchi R, Luo P, Shirasawa S, et al. Lbx1 and Tlx3 are opposing switches in determining GABAergic versus glutamatergic transmitter phenotypes. Nat Neurosci. 2005;8:1510–5. Nov
4. Smits WK, Vermeulen C, Hagelaar R, Kimura S, Vroegindeweij EM, Buijs-Gladdines JGCAM, et al. Elevated enhancer-oncogene contacts and higher oncogene expression levels by recurrent CTCF inactivating mutations in acute T cell leukemia. Cell Rep. 2023;42:112373.
5. Botten GA, Zhang Y, Dudnyk K, Kim YJ, Liu X, Sanders JT, et al. Structural variation cooperates with permissive chromatin to control enhancer hijacking-mediated oncogenic transcription. Blood. 2023;142:336–51.
6. Göös H, Kinnunen M, Salokas K, Tan Z, Liu X, Yadav L, et al. Human transcription factor protein interaction networks. Nat Commun. 2022;13:766.
7. Dadi S, Le Noir S, Payet-Bornet D, Lhermitte L, Zacarias-Cabeza J, Bergeron J, et al. TLX homeodomain oncogenes mediate T cell maturation arrest in T-ALL via interaction with ETS1 and suppression of TCRα gene expression. Cancer Cell. 2012;21:563–76.
8. Shimomura A, Patel D, Wilson SM, Koehler KR, Khanna R, Hashino E. Tlx3 promotes glutamatergic neuronal subtype specification through direct interactions with the chromatin modifier CBP. PLoS ONE. 2015;10:10.
9. Renou L, Boelle P, Deswarte C, Spicuglia S, Benyoucef A, Calvo J, et al. Homeobox protein TLX3 activates miR-125b expression to promote T-cell acute lymphoblastic leukemia. Blood Adv. 2017;1:733–47.
10. Jennings BH, Ish-Horowicz D. The Groucho/TLE/Grg family of transcriptional corepressors. Genome Biol. 2008;9:205.
11. Palaparti A, Baratz A, Stifani S. The Groucho/transducin-like enhancer of split transcriptional repressors interact with the genetically defined amino-terminal silencing domain of histone H3. J Biol Chem. 1997;272:26604–10.
12. Chen G, Fernandez J, Mische S, Courey AJ. A functional interaction between the histone deacetylase Rpd3 and the corepressor groucho in Drosophila development. Genes Dev. 1999;13:2218–30.
13. Yu X, Li P, Roeder RG, Wang Z. Inhibition of androgen receptor-mediated transcription by amino-terminal enhancer of split. Mol Cell Biol. 2001;21:4614–25.
14. Daniels DL, Weis WI. Beta-catenin directly displaces Groucho/TLE repressors from Tcf/Lef in Wnt-mediated transcription activation. Nat Struct Mol Biol. 2005;12:364–71.
15. Cai Y, Brophy PD, Levitan I, Stifani S, Dressler GR. Groucho suppresses Pax2 transactivation by inhibition of JNK-mediated phosphorylation. EMBO J. 2003;22:5522–9. Oct 15
16. Riz I, Lee HJ, Baxter KK, Behnam R, Hawley TS, Hawley RG. Transcriptional activation by TLX1/HOX11 involves Gro/TLE corepressors. Biochem Biophys Res Commun. 2009;380:361. Mar 6
17. Liu Y, Easton J, Shao Y, Maciaszek J, Wang Z, Wilkinson MR, et al. The genomic landscape of pediatric and young adult T-lineage acute lymphoblastic leukemia. Nat Genet. 2017;49:1211–8.
18. Touzart A, Mayakonda A, Smith C, Hey J, Toth R, Cieslak A, et al. Epigenetic analysis of patients with T-ALL identifies poor outcomes and a hypomethylating agent-responsive subgroup. Sci Transl Med. 2021;13:eabc4834.
19. Bornschein S, Demeyer S, Stirparo R, Gielen O, Vicente C, Geerdens E, et al. Defining the molecular basis of oncogenic cooperation between TAL1 expression and Pten deletion in T-ALL using a novel pro-T-cell model system. Leukemia. 2018;32:941.
20. Palomero T, Wei KL, Odom DT, Sulis ML, Real PJ, Margolin A, et al. NOTCH1 directly regulates c-MYC and activates a feed-forward-loop transcriptional network promoting leukemic cell growth. Proc Natl Acad Sci USA. 2006;103:18261–6.
21. Bonnet M, Loosveld M, Montpellier B, Navarro JM, Quilichini B, Picard C, et al. Posttranscriptional deregulation of MYC via PTEN constitutes a major alternative pathway of MYC activation in T-cell acute lymphoblastic leukemia. Blood. 2011;117:6650–9.
22. Herranz D, Ambesi-Impiombato A, Palomero T, Schnell SA, Belver L, Wendorff AA, et al. A NOTCH1-driven MYC enhancer promotes T cell development, transformation and acute lymphoblastic leukemia. Nat Med. 2014;20:1130–7.
23. Staal FJT, Weerkamp F, Langerak AW, Hendriks RW, Clevers HC. Transcriptional control of t lymphocyte differentiation. Stem Cells. 2001;19:165–79.
24. Zhang Y, Qian JJ, Zhou YL, Huang X, Li JH, Li XY, et al. Comparison of early T-cell precursor and non-ETP subtypes among 122 Chinese adults with acute lymphoblastic leukemia. Front Oncol. 2020;10:1423.
25. Van Thillo Q, De Bie J, Seneviratne JA, Demeyer S, Omari S, Balachandran A, et al. Oncogenic cooperation between TCF7-SPI1 and NRAS(G12D) requires β-catenin activity to drive T-cell acute lymphoblastic leukemia. Nat Commun. 2021;12:4164.
26. Brady SW, Roberts KG, Gu Z, Shi L, Pounds S, Pei D, et al. The genomic landscape of pediatric acute lymphoblastic leukemia. Nat Genet. 2022;54:1376–89.
27. de Bock CE, Demeyer S, Degryse S, Verbeke D, Sweron B, Gielen O, et al. HOXA9 cooperates with activated JAK/STAT signaling to drive leukemia development. Cancer Discov. 2018;8:616–31.
28. Thielemans N, Demeyer S, Mentens N, Gielen O, Provost S, Cools J. TAL1 cooperates with PI3K/AKT pathway activation in T-cell acute lymphoblastic leukemia. Haematologica. 2022;107:2304–17.
29. Tsherniak A, Vazquez F, Montgomery PG, Weir BA, Kryukov G, Cowley GS, et al. Defining a cancer dependency map. Cell. 2017;170:564–576.e16.
30. Coustan-Smith E, Mullighan CG, Onciu M, Behm FG, Raimondi SC, Pei D, et al. Early T-cell precursor leukaemia: a subtype of very high-risk acute lymphoblastic leukaemia. Lancet Oncol. 2009;10:147–56.
31. Copley RR. The EH1 motif in metazoan transcription factors. BMC Genom. 2005;6:169.
32. Shimeld SM. A transcriptional modification motif encoded by homeobox and fork head genes. FEBS Lett. 1997;410:124–5.

33. Gehre N, Nusser A, von Muenchow L, Tussiwand R, Engdahl C, Capoferri G, et al. A stromal cell free culture system generates mouse pro-T cells that can reconstitute T-cell compartments in vivo. Eur J Immunol. 2015;45:932–42.
34. Schmidl C, Rendeiro AF, Sheffield NC, Bock C. ChIPmentation: fast, robust, low-input ChIP-seq for histones and transcription factors. Nat Methods. 2015;12:963–5.

ACKNOWLEDGEMENTS

We thank Dr Thomas Müller from the Max-Delbrück-Centrum of Molecular Medicine (MDC) in Berlin for kindly providing us with the custom made TLX3 antibody. We thank the VIB flow cytometry core and KU Leuven genomics core for the support in processing the data obtained during this study. The graphical abstract was created using BioRender.com. This work was supported by a FWO fellowship to QVT, a postdoctoral fellowship to SD by the Foundation against Cancer, a postdoctoral FWO fellowship to AV, and a research grant by FWO to JC.

AUTHOR CONTRIBUTIONS

LL and QVT designed and performed experiments, analyzed and interpreted data; NM, SP, OG, LB, and KJ performed experiments; SD performed bioinformatics analyses; AV and JC jointly coordinated the study; CDB involved in scientific discussions and review of the manuscript; GA and VA provided T-ALL adult patient data from GRAALL03/05 and were involved in scientific discussions; LL, QVT, and AV wrote the manuscript. All authors critically read and contributed to the final version of the manuscript.

COMPETING INTERESTS

This work was supported by a FWO fellowship to QVT, a postdoctoral fellowship to SD by the Foundation against Cancer, a postdoctoral fellowship to AV by the FWO, and a research grant by FWO to JC.

ADDITIONAL INFORMATION

Supplementary information The online version contains supplementary material available at https://doi.org/10.1038/s41375-025-02513-w.

Correspondence and requests for materials should be addressed to Jan Cools or Alexandra Veloso.